Automated Pick-Place of Silicon Nanowires

Xutao Ye*, Yong Zhang*, Changhai Ru, Jun Luo, Shaorong Xie, and Yu Sun

***Abstract*—Pick-place of single nanowires inside scanning electron microscopes (SEM) is useful for prototyping functional devices and characterizing nanowires's properties. Nanowire pick-place has been typically performed via teleoperation, which is time-consuming and highly skill-dependent. This paper presents an automated approach to the pick-place of single nanowires. Through SEM visual detection and vision-based motion control, the system automatically transferred individual silicon nanowires from their growth substrate to a microelectromechanical systems (MEMS) device that characterized the nanowires's electromechanical properties. The performance of the nanorobotic pick-up and placement procedures was experimentally quantified.**

***Note to Practitioners*—Manipulation of single nanowires or nanotubes is important for their characterization and nanodevice construction. Joystick-based teleoperation of nanomanipulators installed inside a SEM is a commonly used approach for the pick-place of individual nanowires/nanotubes. Nevertheless, the manual process is tedious and time-consuming, even for skilled operators. To address this issue, this paper presents a set of SEM-vision-based techniques to automate the nanowire pick-place process. The techniques can facilitate nanowire/nanotube property characterization and nanodevice prototyping.**

***Index Terms*—Automated nanomanipulation, nanorobotic pick-place, nanowires, scanning electron microscopes (SEM).**

I. Introduction

ADVANCES in nanomaterial synthesis have resulted in a plethora of one-dimensional nanomaterials (i.e., nanowires and nanotubes) that exhibit interesting mechanical, electronic, electromechanical, or optical properties. Nanomaterial synthesis produces a high number of nanomaterials *en masse*. The characterization of a single nanomaterial requires the isolation and manipulation of individual nanomaterials. In addition, prototyping functional devices using single nanomaterials also requires individual nanomaterial manipulation.

Several nanowire/nanotube manipulation techniques have been developed, such as direct synthesis [1], dielectrophoresis [2], [3], contact printing [4], [5], and pick-place [6]–[8]. Of these techniques, nanomaterial pick-place offers high specificity and precision that other techniques lack, although it is a serial and slower process. By virtue of this advantage, pick-place has been employed for nanowire/nanotube property characterization and also for nanodevice assembly.

For instance, a zinc oxide nanowire was picked up from its growth substrate and placed across source-drain electrodes to form a field-effect transistor as an ultra-sensitive biosensor and gas sensor [9]. Carbon nanotubes [10], silicon nanowires [11], [12], and vanadium dioxide nanowires [13] were also individually picked up and placed onto microelectromechanical systems (MEMS) devices for mechanical or electromechanical characterization.

Thus far, nanowire/nanotube pick-place has been performed via teleoperation [11], [12], where an operator carefully monitors an scanning electron microscope (SEM) screen and operates joysticks to control nanomanipulators inside the SEM. High-resolution visual feedback from SEM provides the operator with accurate relative XY positions between nanomanipulators, nanowires, and target placement locations. Besides nanowire pick-place, other types of nanomanipulation (e.g., stretching, compressing, cutting, pushing, and pulling of materials) have also been performed in SEM [14]–[20], also taking advantage of the imaging capability of SEM over optical microscopy. For example, helical nanobelts were stretched in an SEM to characterize their linear-to-rotary motion conversion behavior [17]. Mechanical characterization and cutting of cells have also been demonstrated in an environmental SEM [20]. Despite the aforementioned unique capabilities, SEM nanomanipulation realized by manual operation is time consuming and highly skill dependent, and has low productivity, demanding the development of robotic techniques to facilitate the nanomanipulation processes.

Nanorobotic manipulation involves visual detection of nanomaterials, visually tracking and controlling end-effectors, and the determination of vertical positions of end-effectors relative to the nanomaterials to manipulate. The active contour, Hough transform, and principle component analysis were applied to the detection of carbon nanotubes [21]. Feature-based methods [22] and correlation-based methods [23] have also been implemented for visual tracking of end-effectors in nanomanipulation. Based on visual tracking, a visual servo control system was also constructed for automated probing of nanowires [18].

Techniques were also developed for detecting vertical positions of end-effectors, using SEM vision or touch sensors.

Manuscript received September 09, 2012; revised December 09, 2012; accepted January 19, 2013. Date of publication March 07, 2013; date of current version June 27, 2013. This paper was recommended for publication by Associate Editor P. Lutz and Editor K. Bohringer upon evaluation of the reviewers' comments. This work was supported by the Natural Sciences and Engineering Research Council of Canada under a Collaborative Research and Development Grant, by the Ontario Centers of Excellence under a Collaborative Research Grant, by Hitachi High-Technologies Canada Inc., by the Canada Research Chairs Program, by Canadian Microelectronics Corporation under a Financial Assistance Program for Microfabrication, and by the National Natural Science Foundation of China (#61233010). *Asterisk indicates authors contributed equally.*

X. Ye and Y. Sun are with the Department of Mechanical and Industrial Engineering, University of Toronto, Toronto, ON M5S 3G8, Canada (e-mail: xutao.ye@utoronto.ca; sun@mie.utoronto.ca).

Y. Zhang is with the School of Aerospace Engineering, Georgia Institute of Technology, Atlanta, GA 30332 USA (e-mail: yong.zhang@aerospace.gatech.edu).

C. Ru is with the College of Automation, Harbin Engineering University, Harbin 150001, China (e-mail: changhai.ru@utoronto.ca).

J. Luo and S. Xie are with the School of Mechatronic Engineering and Automation, Shanghai University, Shanghai 200072, China (e-mail: luojun@shu.edu.cn; srxie@shu.edu.cn).

Color versions of one or more of the figures in this paper are available online at http://ieeexplore.ieee.org.

Digital Object Identifier 10.1109/TASE.2013.2244082

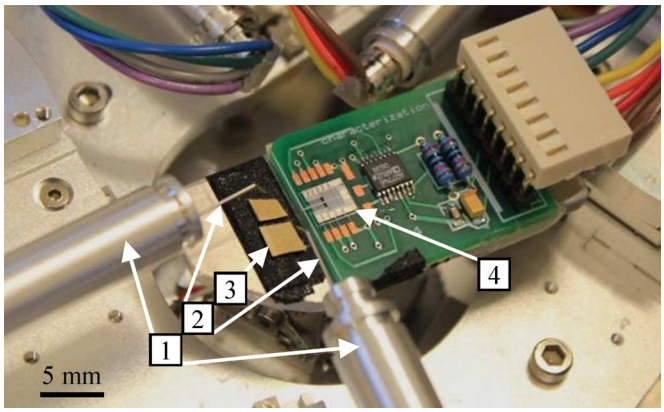

Fig. 1. Experimental setup: a nanomanipulation system and a MEMS nanowire-testing device are installed inside an SEM: 1. nanomanipulators; 2. probes; 3. nanowire growth substrate; and 4. MEMS device.

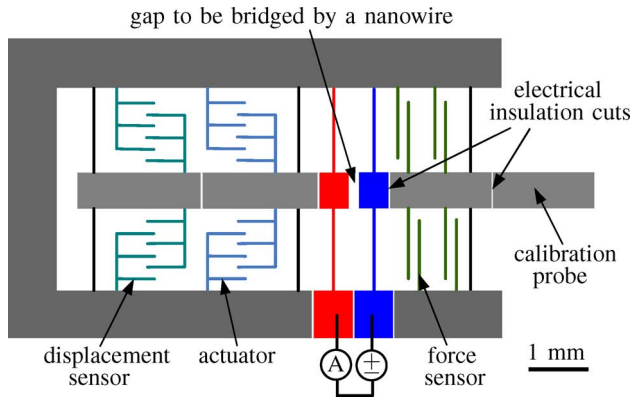

Fig. 2. MEMS device for electromechanical characterization of nanowires.

For instance, when an end-effector is lowered to approach a substrate surface, its shadow appears, roughly indicating the proximity [21], [24]. After the end-effector contacts the substrate, its sliding behavior is an accurate indicator of the contact between the end-effector and the substrate surface [18], [25], [26]. In addition, MEMS displacement/force sensors can also be used for contact detection [27], [28]. Nonetheless, those methods are limited to detecting contact between an end-effector and a substrate, hence not applicable to the detection of end-effector-nanowire contact, which is required for automated nanowire pick-up.

Viewing the end-effector-nanowire setup from a different angle provides depth information. It can be realized by tilting the SEM's electron beam [29] or specimen stage [30], or using a dual-beam SEM-FIB (focused ion beam) instrument [8]. However, these approaches are not applicable to standard SEM and require the development of complex three-dimensional reconstruction algorithms.

In this paper, we report automation techniques for automated pick-place of individual nanowires. The pick-place technique reported in this paper requires only a standard SEM without relying on FIB assistance [12]. SEM visual feedback is processed to automatically select suitable nanowires for pick-place, automatically bring a probe into contact with a target nanowire for pick-up, and automatically place the picked-up nanowire to a target location regardless of the vertical orientation of the nanowire. We also demonstrate automated transfer of single nanowires onto a MEMS structure for mechanical and electrical characterization, as an application of the automated nanowire pick-place technique. The MEMS device is briefly introduced in this paper for clarity and self-containment. Details of the design, fabrication, and operation of the device can be found in [11].

II. System and Techniques

A. Experimental Setup

A nanomanipulation system (Zyvex S100) and a MEMS testing device were installed to the specimen stage of an SEM (Hitachi S-4000), as shown in Fig. 1. The nanomanipulation system has four quadrants of three-degrees-of-freedom nanomanipulators, each consisting of a coarse-positioning stage and a fine-positioning unit. The coarse-positioning stage contains three identical piezoelectric slip-stick motors, each having a travel of 12 mm with 100-nm resolution. The fine-positioning unit contains a piezoelectric tube having travel ranges of 10 μm along the axis of the tube and 100 μm along each of the two transverse directions with 5-nm resolution. The nanomanipulators do not have integrated position sensors for either coarse or fine positioning, as in most nanomanipulation systems.

Each of the two nanomanipulators carries a tungsten probe (probe tip diameter: 200 nm) as an end-effector for manipulating nanowires. The probes were chemically cleaned to remove the native tungsten oxide using KOH solutions and HF before being mounted onto the nanomanipulators. A silicon nanowire substrate is placed close to the MEMS device. The nanowires were vapor-liquid-solid synthesized using low pressure chemical vapor deposition.

The MEMS device (Fig. 2) is composed of two suspended shuttles, namely, the actuator shuttle (on the left) and the force sensor shuttle (on the right), with a small gap (5 μm in width) in between to be bridged by a nanowire specimen. The actuator shuttle includes an electrostatic actuator and a capacitive displacement sensor that measures displacements of the actuator. The force sensor shuttle contains a capacitive force sensor, which measures tensile forces of the specimen as well as its own displacement. When the actuator shuttle moves leftward, the specimen is stretched and the force sensor shuttle is also pulled leftward. Thus, the amount of specimen elongation is the displacement of the actuator subtracted by that of the force sensor. During the tensile stretching, a voltage can be applied between the two suspended electrodes interfacing the nanowire, yielding current-voltage (I-V) curves at different strain levels.

To transfer a nanowire to the MEMS device, the nanorobotic system detects individual nanowires on the growth substrate (Section II-B), picks up one nanowire (Section II-C), and places it across the gap of the MEMS device (Section II-D), followed by electromechanical testing.

B. Detection and Selection of Nanowires

Fig. 3(a) shows an edge region on the nanowire growth substrate. It can be observed that only nanowires protruding

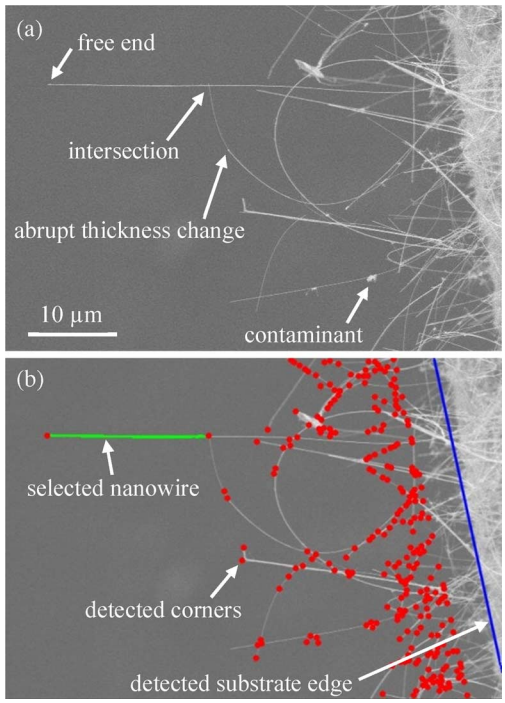

Fig. 3. Nanowire detection. (a) Image shows a network of nanowires protruding out from the growth substrate edge. (b) Image processing result: a nanowire segment is selected by the system after the corners in the nanowire network are detected.

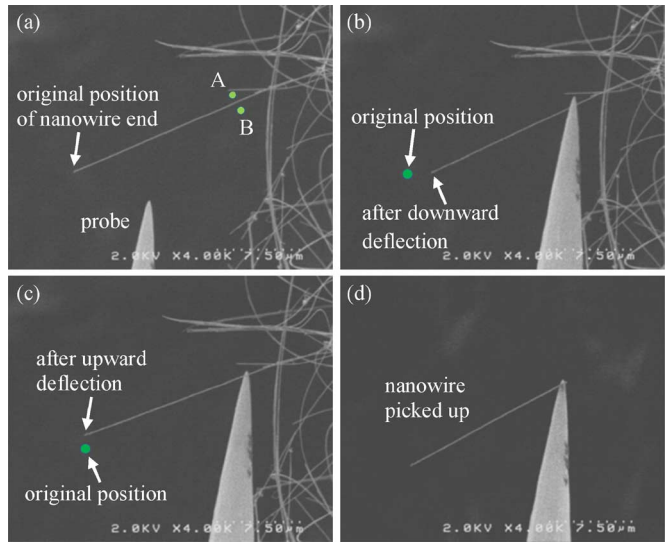

Fig. 4. Nanowire pick-up. (a) A probe is brought close to a nanowire. (b) The probe descends and contacts the nanowire. (c) The probe descends underneath the nanowire and ascends to contact it. (d) The nanowire is EBID-soldered to the probe and picked up.

out from the substrate edge contain sparse nanowires, whereas nanowires within the substrate are dense and tangled and not individually accessible. Furthermore, not all protruding nanowires are suitable for pick-place. As shown in Fig. 3(a), many nanowires are connected or entangled to other nanowires, or spatially intersect, which may cause entanglement during pick-up. Some nanowires have contaminants on them that may make placing the nanowire on a surface difficult and can undesirably affect characterization results. There are also cases that two nanowires are bound together and appear as a single nanowire except that they exhibit abrupt thickness changes at the double-to-single transition.

Based on the above observations, the criteria for selecting a suitable nanowire are defined as follows: 1) it must be a single nanowire that has one end freely suspended and 2) between the free end and its nearest contaminant or intersection on the nanowire, the length must be larger than 10 μm to ensure that this clean section of the nanowire is able to span the 5 μm gap on the MEMS device.

For the system to automatically select suitable nanowires, the following image processing procedure was developed. A low-pass Gaussian filter is applied to divide the image into two regions having respectively sparse and dense nanowires in order to detect the substrate edge. Subsequently, edge detection between the two regions and Hough line transform are performed to determine the angle and position of the substrate edge. At a distance away from the edge in the sparse region, Gaussian filtering and adaptive thresholding are used to obtain the overall contour of the nanowire network.

Subsequently, corner detection is employed to detect free ends of nanowires, nanowire intersections, contaminants on nanowires, and abrupt changes of nanowire thickness. The detected corners separate the connected contour into individual contours, each of which represents a nanowire segment. The minimum bounding rectangle of a nanowire segment is used to approximate the length and straightness of that segment. Nanowires with one free end are distinguished from the rest of the nanowires by checking both ends of each segment to determine whether they are connected to or near other nanowire segments. As a result, the nanowire segments with one free end and sufficient length and straightness are selected, with their positions recorded. In order to obtain the locations of all suitable nanowires from the entire substrate edge, the system moves the specimen stage along the direction of the substrate edge by steps for SEM imaging.

C. Pick-Up of Nanowires

A probe is brought close to a section of the substrate edge that contains a selected nanowire [Fig. 4(a)]. To affix the nanowire to the probe tip for pick-up, the probe needs to contact the nanowire near its root from underneath. In Fig. 4(a), points A and B at either side of the nanowire near its root are determined in the image frame by the system as the target positions of the probe tip. To recognize the probe from Fig. 4(a), image erosion is applied to remove the nanowire network as thin features, leaving only the eroded image of the probe. Contour recognition is then applied to the probe region in the original image, yielding the position of the probe tip as the highest point of the probe contour. The probe image is also stored and used as a template for visual tracking using the sum-of-squared-differences (SSD) algorithm. The magnification of the SEM is maintained at $4,000\times$, which is appropriate for both pick-up and placement procedures. The probe template obtained here is used throughout the entire pick-place process for visual tracking.

The drift of SEM imaging should be accounted for in visual tracking. Image drift refers to the movement of the entire image,

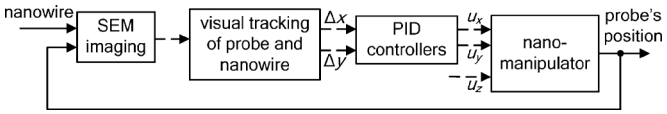

Fig. 5. The probe is visually servoed to either move in XY (Z axis actuation voltage u_z remains constant) or descend (u_z increases) with the induced xy position shifts compensated for.

caused by electron beam drift, charge drift on the specimen, and electromagnetic interferences from the environment and the nanomanipulators. To remove the effect of image drift on visual tracking, a stationary feature in the image is simultaneously visually tracked and used as a position reference.

The probe is visually servoed in the XY plane (Fig. 5 with Z axis actuation voltage u_z being constant) to arrive at point A from above the nanowire. The system then continuously lowers the probe at a preset constant speed (e.g., 2 μm) to approach the nanowire. Owing to the perspective projection model of SEM, the probe's Z position change induces its xy position shift in the image frame, causing the probe to stray away from point A. In order to maintain the probe's xy position in the image frame, the system adjusts the probe's XY position in the world frame to compensate for the xy shift, also via visual servo control (Fig. 5 with u_z increasing for probe descending). The PID parameters in the control system are experimentally tuned through trial and error.

The probe tip then contacts the nanowire, causing it to deflect downward [Fig. 4(b)]. By visually tracking the free end of the nanowire until its displacement surpasses a threshold value (e.g., 0.5 μm), the system detects this contact event and halts the probe. It can be noticed that the system does not acquire or monitor the actual vertical distance between the probe and the nanowire during the probe descending process. Only at the moment the probe tip bends the nanowire is the system able to determine that they are at the same height and in contact.

The system then raises the probe by a certain height (e.g., 2 μm), to overcome the adhesion from the nanowire and detach from it. The probe is then visually servoed to arrive at point B and descends by a certain height (e.g., 7 μm) to locate itself below the nanowire. The probe is visually servoed to arrive at point A again and raised to contact the nanowire. By tracking the free end of the nanowire, the upward deflection caused by the probe-nanowire contact is detected [Fig. 4(c)]. It is a must for the probe to form contact with the nanowire from underneath since the electron beam must irradiate both the nanowire and the probe for electron-beam induced deposition (EBID) soldering [31]. When the probe is located above the nanowire, the probe blocks the nanowire from the electron beam irradiation, making EBID soldering infeasible. After the EBID soldering, the probe is retracted to detach the nanowire from the growth substrate [Fig. 4(d)].

D. Placement of Nanowires

The picked-up nanowire is transferred by the nanomanipulator to above the gap on the MEMS device [Fig. 6(a)]. The probe [probe 1 in Fig. 6(a)] is recognized via template matching using the probe template obtained from Fig. 4(a). The Hough transform is applied to recognize the edges of the gap on the

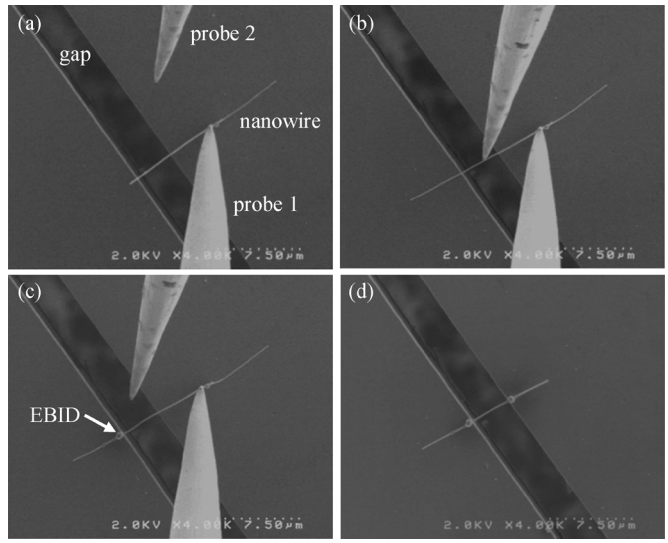

Fig. 6. Nanowire placement. (a) Probe 1 positions the nanowire over the gap of the device, followed by the probe's landing on the device. (b) Probe 2 pushes the nanowire into contact with the device. (c) The nanowire is EBID-soldered to the left edge of the gap, followed by the retraction of probe 2. (d) The nanowire is EBID-soldered to the right edge of the gap, followed by the electrical breakdown of the nanowire between the second EBID point and probe 1 for the retraction of probe 1.

MEMS device as two parallel lines. After the exclusion of probe 1 and two gap edges, contour recognition is used to recognize the nanowire and probe 2. By comparing the areas within the contours, the nanowire and probe 2 are distinguished from each other. Since the section of the nanowire on the right side of the probe has experienced tensile fracture due to the detachment of this nanowire from its growth substrate, the left section of the nanowire is intact and should be used for obtaining valid characterization results. The left end of the nanowire is recognized as the leftmost point of the nanowire's contour.

The system visually servos the left end of the nanowire to arrive at a point at a certain distance (e.g., 1 μm) to the left of the left edge of the gap on the MEMS device, to achieve an overlap between the nanowire and the left electrode of the device. The system descends the probe while visually tracking both the probe tip and the left end of the nanowire. During descending, when the left end of the nanowire deviates from its original xy position in the image frame by a certain threshold (e.g., 0.5 μm), the system pauses the descending and visually servos the probe and the nanowire to return to their original xy positions, to maintain a proper overlap between the nanowire with the left electrode. The reason that the probe is not visually servoed constantly to remain at its xy position is that it would interfere with the detection of contact between the probe/nanowire with the MEMS device surface.

Depending on the nanowire's vertical orientation, either the probe or the nanowire lands on the device first. If the nanowire protrudes upward from the probe tip, the probe comes into contact with the device, with the nanowire still above the device without contacting the MEMS device surface. If the nanowire protrudes downward from the probe tip, the nanowire comes into contact with the device first. The system determines which of these two scenarios occurs and applies corresponding techniques.

If the probe lands first, it slides forward after the contact owing to its flexibility, inducing abrupt changes of the probe's moving speed and direction in the image frame. By monitoring the probe's movement over a few consecutive image frames, the system determines that contact has occurred and halts the probe. The system then uses the second probe [probe 2 in Fig. 6(a)] to push the nanowire into contact with the device [Fig. 6(b)]. Before bringing probe 2 to the nanowire, the system needs to position it at a certain height above the MEMS device.

Probe 2 is visually tracked while being lowered to contact the device. The system detects probe sliding and then raises the probe to a certain height (e.g., $\sim$10 μm) above the MEMS device. A point on the portion of the nanowire within the gap (e.g., 1 μm away from the intersection of the nanowire and the right edge of the gap) is determined by the system as the target xy position of the probe. The system visually servos the probe to arrive at this target position, and lowers the probe to the height of the device surface so as to press the nanowire down to the device.

EBID is used to solder the nanowire to the left edge of the gap, followed by the retraction of the second probe [Fig. 6(c)]. The system detects the angle between the nanowire and the gap, and visually servos the probe to track an arc with the EBID point as the center so as to orient the nanowire to be perpendicular to the gap. The nanowire is EBID-soldered to the right edge of the gap. To detach the probe from the nanowire, an increasing voltage is applied between the probe and the right electrode of the device to electrically break down the nanowire between the second EBID point and the probe, followed by the probe retraction [Fig. 6(d)].

For the second case where the nanowire lands first onto the MEMS device, the nanowire either adheres to or slides on the device after contact, inducing the distance change between the left end of the nanowire and the probe tip. The system detects this distance change and determines that the nanowire has landed first. The system continues to lower the probe until it slides on the device. The nanowire is EBID-soldered to the left edge of the gap, subsequently oriented to be perpendicular to the gap, and soldered to the right edge of the gap, followed by probe retraction after the electrical breakdown of the nanowire. Apparently, the second probe is not needed for this case.

III. Experimental Results and Discussions

A. Nanowire Pick-Up

1) Probe-Nanowire Contact Detection: For the detection of contact between the probe and the nanowire to be picked up, the system starts to visually track the free end of the nanowire when starting to lower the probe. Tracking results are shown in Fig. 7. In segment AB, the probe was descending by steps of 50 nm prior to contacting the nanowire. The displacement variation of the nanowire end was approximately 2 pixels, stemming from image noises. Given this variation level, the threshold for contact detection was set to 10 pixels in experiments.

At point B, the probe established contact with the nanowire. Subsequently, the next descending step resulted in a nanowire displacement of 5.8 pixels. The following step brought the nanowire end to point C, with a total displacement of 15.0 pixels from point B. Since the threshold was surpassed, the system detected the contact and halted the probe. The probe stayed there for 1 s, corresponding to segment CD. The purpose of this pause was only for clearly showing segments CD and DE, thus unnecessary for contact detection. At point D, the system started to raise the probe to 2 μm above the nanowire.

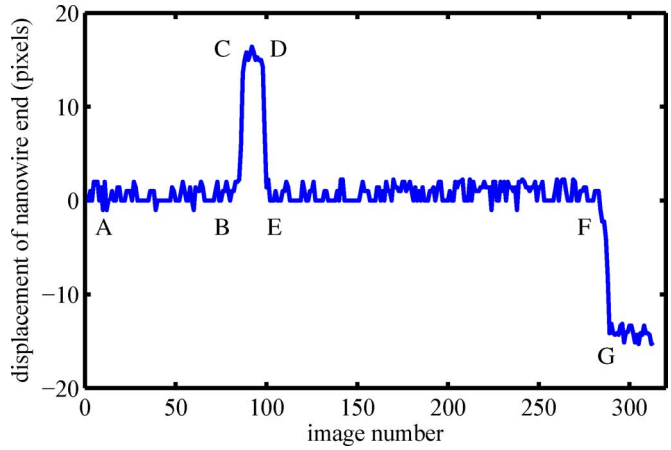

Fig. 7. Visual tracking of the free end of nanowire for detecting contact between the probe and the nanowire.

The nanowire separated from the probe at its original position (point E), rather than followed the probe further by adhesion forces. It should be noted that some nanowires were indeed drawn up by the probe, resulting in the displacement of the nanowire tip in the opposite direction. The system lowered the probe, inserted it below the nanowire, and raised it to contact the nanowire. At point F, contact was established and the nanowire started to be deflected upward. At point G, the nanowire displacement exceeded the threshold, completing contact detection followed by EBID-soldering.

2) Nanowire Pick-Up: To quantify the reproducibility of the pick-up procedure, trials were performed on ten nanowires selected by the system according to the methodology described in Section II-B. The nanowires were at different locations on the substrate edge, and varied in vertical and horizontal protruding angles, length (12.7–20.5 μm), and diameter (74–113 nm), thus representing different pick-up circumstances in terms of the complexity of surrounding nanowire networks and the orientation and flexibility of the target nanowire. The system successfully picked up eight of those ten nanowires.

Out of the two failure cases, one nanowire (16.4 μm in length and 96 nm in width) suddenly disappeared from the image when the probe contacted it from above. We speculate that the electric charges accumulated on the nanowire from e-beam irradiation caused a breakdown current to pass between the nanowire and the probe upon their contact, causing the nanowire to fracture and fall. The tungsten probe does not charge from e-beam irradiation since it has been stripped of its surface oxide and has been grounded. Shortening the time of e-beam imaging on the nanowire prior to pick-up or decreasing the SEM acceleration voltage might be helpful in reducing the accumulated charges before the probe-nanowire contact.

The other nanowire (15.3 μm in length and 74 nm in width) kept adhering to the probe by adhesion forces when the probe

moved upward after contacting it from above. This nanowire separated from the probe at some point when its internal bending force overcame the adhesion forces from the probe. When it bounced back and overshot, its suspended end was entangled to the surrounding nanowires. It was observed that thinner nanowires were more likely to be drawn up by the probe via adhesion because of their low bending stiffness, and hence were more likely to be entangled if they were also closely surrounded by other nanowires. This type of failure may be mitigated by horizontally sliding the probe along the nanowire (rather than raising the probe) until it separates from the suspended end of the nanowire.

For each of the eight successful cases, the pick-up procedure was attempted 15 times on the nanowire before the final EBID-soldering was conducted. Each time after the probe contacted the nanowire from below and was ready for EBID, it was retracted and brought to a different starting XYZ position for the next trial. The system successfully completed all the trials, resulting in a 100% repeatability ($n = 120$). This set of experiments demonstrated the reliability of the image processing and motion control techniques against random noises and drift of SEM imaging and against variations in initial conditions.

B. Nanowire Placement

To quantify the reproducibility of the placement procedure, the system conducted trials on five of the picked-up nanowires to place them onto the MEMS device. These nanowires had different horizontal orientations relative to the probe and also the gap of the device. From the nanowire/probe landing, the system determined the vertical orientations of the nanowires: four protruded upward from the probe tip and one protruded downward. The system successfully placed all of the five nanowires including the final probe retraction.

Prior to nanowire pick-up, the vertical orientation of a nanowire is difficult to detect from SEM imaging, particularly if the nanowire is nearly horizontal. This challenge was addressed by this nanorobotic manipulation system during nanowire placement. The system detected the vertical orientation of a nanowire when landing the probe and the nanowire onto the device. Furthermore, the system was able to place a nanowire even if it turned out that the nanowire protruded upward.

C. Nanowire Characterization

Each of the five placed nanowire was tensile-stretched until its fracture with the force-elongation data recorded, during which its I-V data curves were also obtained using a SourceMeter (Keithley 2602) at a number of strain levels. A representative stress-strain curve from one nanowire is shown in Fig. 8(a), yielding the Young's modulus (165.3 GPa) and failure strength (5.67 GPa). The Young's modulus derived from five silicon nanowires was 165.4 ± 3.9 GPa ($n = 5$), in agreement with findings for VLS-grown [111] silicon nanowires reported previously [32], [33]. The failure strengths of the nanowires were determined to be 5.3 ± 0.6 GPa ($n = 5$).

For coupled electrical characterization at each strain level, a voltage sweep (e.g., from -20 V to $+20$ V) was applied to a nanowire specimen and the current flow was measured.

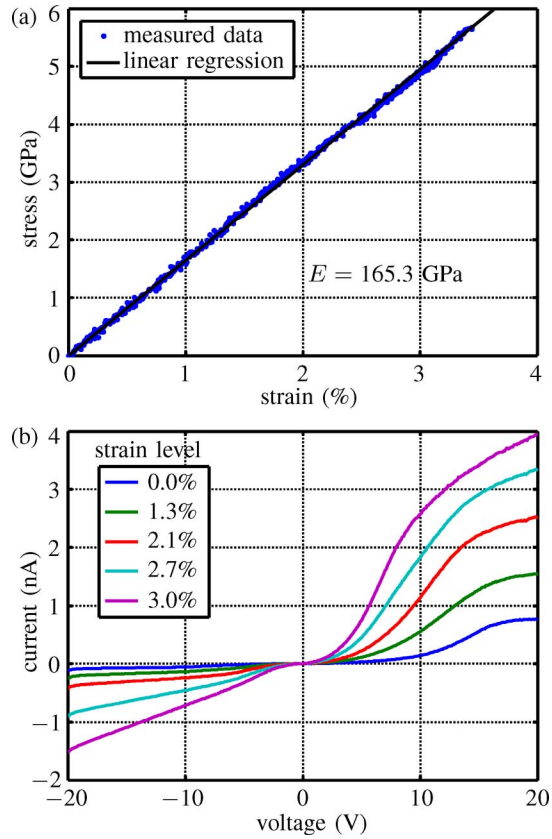

Fig. 8. Mechanical and electrical characterization results. (a) Stress-strain curve. (b) I-V characteristics of the nanowire under different strain levels.

Fig. 8(b) shows I-V characteristics of a silicon nanowire at different strain levels. It can be seen that straining the nanowire resulted in I-V changes, indicating the piezoresistive effect. The slope of the linear portion of a I-V curve at high voltages approximates the conductance of the specimen [34], [35]. Therefore, the voltage range of 5–9 V in Fig. 8(b) was used to determine the intrinsic resistance of the nanowire at different strain levels. The resistance and resistivity under the unstrained condition were determined to be $5.9 \times 10^{11}\Omega$ and 406 $\Omega \cdot$ m. At 3.0% strain, the resistance was determined to be $2.2 \times 10^{10}\Omega$, reduced by a factor of 26.8 from the resistance at zero strain. The gauge factor (ratio of relative resistance change to strain) of the nanowire was determined to be 67.1 at 1.3% strain.

D. Discussion

Automated detection of nanowires by our system significantly reduced the detection time to approximately 3 min (versus over 30 min in manual detection which involves carefully observing the SEM screen and adjusting the focus). Automated nanowire contact detection not only speeds up the process but also avoids undesired destruction of nanowires due to delays in human responses as in teleoperation. Without considering the time for EBID, which does not require human or system monitoring, the entire automated pick-place procedure takes approximately 10 min, whereas a skilled human operator needs longer than 2 h.

Probes used in this work are single-ended end-effectors for nanomanipulation. Besides nano probes, grippers with double

tips have also been demonstrated for the manipulation of nanoobjects. For instance, a MEMS gripper with thin gripping tips was used to pick and place nanospheres [24]. A gripper was also used to pick up vertically aligned carbon nanotubes [36]. In comparison with single-ended probes, grippers are capable of picking up a nanoobject via the application of gripping forces, obviating the need for soldering (e.g., EBID) or gluing a nanoobject onto the end-effector. However, gripping tips typically are much bulkier than probe tips and require precise orientation adjustment in relation to a target nanoobject. In addition, the actuation voltages for opening and closing gripping arms could deflect the electron beam and induce image distortion and drift, complicating vision-based control. Our experiments confirmed that single-ended probes are more dexterous than gripping tips for the task of manipulating one-dimensional nanomaterials such as nanowires.

IV. Conclusion

A nanorobotic system was developed that realized automated pick-place of individual nanowires. The system selected suitable nanowires from the growth substrate, picked a nanowire up, and placed it onto the MEMS device. Vision-based methods were used for detecting the contact between the probe, the nanowire, and the device. The system demonstrated high reproducibility in both the pick-up procedure and the placement procedure. The techniques can facilitate nanomaterial property characterization and nanodevice prototyping.

References

[1] R. He and P. Yang, "Giant piezoresistance effect in silicon nanowires," *Nat. Nanotechnol.*, vol. 1, no. 1, pp. 42–46, Oct. 2006.

[2] D. Xu, A. Subramanian, L. Dong, and B. J. Nelson, "Shaping nanoelectrodes for high-precision dielectrophoretic assembly of carbon nanotubes," *IEEE Trans. Nanotechnol.*, vol. 8, no. 4, pp. 449–456, Jul. 2009.

[3] J. Brown, A. Baca, K. Bertness, D. Dikin, R. Ruoff, and V. Bright, "Tensile measurement of single crystal gallium nitride nanowires on MEMS test stages," *Sens. Actuators, A*, vol. 166, no. 2, pp. 177–186, Apr. 2011.

[4] Z. Fan, J. C. Ho, Z. A. Jacobson, R. Yerushalmi, R. L. Alley, H. Razavi, and A. Javey, "Wafer-scale assembly of highly ordered semiconductor nanowire arrays by contact printing," *Nano Lett.*, vol. 8, no. 1, pp. 20–25, Jan. 2008.

[5] Y. L. Zhang, J. Li, S. To, Y. Zhang, X. Ye, L. You, and Y. Sun, "Automated nanomanipulation for nanodevice construction," *Nanotechnology*, vol. 23, no. 6, p. 065304, Feb. 2012.

[6] M.-F. Yu, M. J. Dyer, G. D. Skidmore, H. W. Rohrs, X. Lu, K. D. Ausman, J. R. V. Ehr, and R. S. Ruoff, "Three-dimensional manipulation of carbon nanotubes under a scanning electron microscope," *Nanotechnology*, vol. 10, no. 3, pp. 244–252, Sep. 1999.

[7] M.-F. Yu, O. Lourie, O. Lourie, K. Moloni, T. F. Kelly, and R. S. Ruoff, "Strength and breaking mechanism of multiwalled carbon nanotubes under tensile load," *Science*, vol. 287, pp. 637–640, Jan. 2000.

[8] Y. Zhu and H. D. Espinosa, "An electromechanical material testing system for *in situ* electron microscopy and applications," in *Proc. Nat. Acad. Sci.*, Oct. 2005, vol. 102, no. 41, pp. 14 503–14 508.

[9] Y. Hu, J. Zhou, P.-H. Yeh, Z. Li, T.-Y. Wei, and Z. L. Wang, "Supersensitive, fast-response nanowire sensors by using Schottky contacts," *Adv. Mater.*, vol. 22, no. 30, pp. 3327–3332, Aug. 2010.

[10] H. D. Espinosa, Y. Zhu, and N. Moldovan, "Design and operation of a MEMS-based material testing system for nanomechanical characterization," *J. Microelectromech. Syst.*, vol. 16, no. 5, pp. 1219–1231, Oct. 2007.

[11] Y. Zhang, X. Liu, C. Ru, Y. L. Zhang, L. Dong, and Y. Sun, "Piezoresistivity characterization of synthetic silicon nanowires using a MEMS device," *J. Microelectromech. Syst.*, vol. 20, no. 4, pp. 959–967, Aug. 2011.

[12] M. Bartenwerfer and S. Fatikow, "Directed nanorobot-based handling of single nanowires," in *Proc. IEEE Int. Conf. Mecha. Autom.*, Beijing, China, Aug. 2011, pp. 183–188.

[13] H. Guo, K. Chen, Y. Oh, K. Wang, C. Dejoie, S. A. S. Asif, O. L. Warren, Z. W. Shan, J. Wu, and A. M. Minor, "Mechanics and dynamics of the strain-induced M1–M2 structural phase transition in individual VO_2 nanowires," *Nano Lett.*, vol. 11, no. 8, pp. 3207–3213, Aug. 2011.

[14] M.-F. Yu, B. S. Files, S. Arepalli, and R. S. Ruoff, "Tensile loading of ropes of single wall carbon nanotubes and their mechanical properties," *Phys. Rev. Lett.*, vol. 84, no. 24, pp. 5552–5555, Jun. 2000.

[15] M.-F. Yu, B. I. Yakobson, and R. S. Ruoff, "Controlled sliding and pullout of nested shells in individual multiwalled carbon nanotubes," *J. Phys. Chem. B*, vol. 104, no. 37, pp. 8764–8767, Sep. 2000.

[16] G. Hwang, H. Hashimoto, D. J. Bell, L. Dong, B. J. Nelson, and S. Schön, "Piezoresistive InGaAs/GaAs nanosprings with metal connectors," *Nano Lett.*, vol. 9, no. 2, pp. 554–561, Feb. 2009.

[17] L. Dong, L. Zhang, B. E. Kratochvil, K. Shou, and B. J. Nelson, "Dual-chirality helical nanobelts: Linear-to-rotary motion converters for three-dimensional microscopy," *J. Microelectromech. Syst.*, vol. 18, no. 5, pp. 1047–1053, Oct. 2009.

[18] C. Ru, Y. Zhang, Y. Sun, Y. Zhong, X. Sun, D. Hoyle, and I. Cotton, "Automated four-point probe measurement of individual nanowires inside a scanning electron microscope," *IEEE Trans. Nanotechnol.*, vol. 10, no. 4, pp. 674–681, Jul. 2011.

[19] T. Fukuda, M. Nakajima, M. R. Ahmad, Y. Shen, and M. Kojima, "Micro- and nanomechatronics," *IEEE Ind. Electron. Mag.*, vol. 4, no. 4, pp. 13–22, Dec. 2010.

[20] Y. Shen, M. Nakajima, Z. Yang, S. Kojima, M. Homma, and T. Fukuda, "Design and characterization of nanoknife with buffering beam for *in situ* single-cell cutting," *Nanotechnology*, vol. 22, no. 30, p. 305701, Jul. 2012.

[21] V. Eichhorn, S. Fatikow, T. Wortmann, C. Stolle, C. Edeler, D. Jasper, O. Sardan, P. Bøggild, G. Boetsch, C. Canales, and R. Clavel, "Nanolab: A nanorobotic system for automated pick-and-place handling and characterization of CNTs," in *Proc. IEEE Int. Conf. Robot. Autom.*, Kobe, Japan, May 2009, pp. 1826–1831.

[22] T. Sievers and S. Fatikow, "Real-time object tracking for the robot-based nanohandling in a scanning electron microscope," *J. Micromechatron.*, vol. 3, no. 3–4, pp. 267–284, Sep. 2006.

[23] B. E. Kratochvil, L. Dong, and B. J. Nelson, "Real-time rigid-body visual tracking in a scanning electron microscope," *Int. J. Robot. Res.*, vol. 28, no. 4, pp. 498–511, Apr. 2009.

[24] B. K. Chen, Y. Zhang, D. D. Perovic, and Y. Sun, "MEMS microgripper with thin gripping tips," *J. Micromech. Microeng.*, vol. 21, no. 10, p. 105004, Sep. 2011.

[25] Y. Zhang, B. K. Chen, X. Liu, and Y. Sun, "Autonomous robotic pick-and-place of microobjects," *IEEE Trans. Robot.*, vol. 26, no. 1, pp. 200–207, Feb. 2010.

[26] Y. L. Zhang, Y. Zhang, C. Ru, B. K. Chen, and Y. Sun, "A load-lock-compatible nanomanipulation system for scanning electron microscope," *IEEE/ASME Trans. Mechatron.*, vol. 18, no. 1, pp. 230–237, Feb. 2013.

[27] K. Kim, X. Liu, Y. Zhang, and Y. Sun, "Nanonewton force-controlled manipulation of biological cells using a monolithic MEMS microgripper with two-axis force feedback," *J. Micromech. Microeng.*, vol. 18, no. 5, p. 055013, May 2008.

[28] V. Eichhorn, S. Fatikow, T. Wich, C. Dahmen, T. Sievers, K. N. Andersen, K. Carlson, and P. Bøggild, "Depth-detection methods for microgripper based CNT manipulation in a scanning electron microscope," *J. Micro-Nano Mech.*, vol. 4, pp. 27–36, Nov. 2008.

[29] M. Jähnisch and S. Fatikow, "3-D vision feedback for nanohandling monitoring in a scanning electron microscope," *Int. J. Optomechatronics*, vol. 1, no. 1, pp. 4–26, 2007.

[30] F. Marinello, P. Bariani, E. Savio, A. Horsewell, and L. D. Chiffre, "Critical factors in SEM 3D stereo microscopy," *Meas. Sci. Technol.*, vol. 19, no. 6, p. 065705, Jun. 2008.

[31] T. Fukuda, M. Nakajima, P. Liu, and H. ElShimy, "Nanofabrication, nanoinstrumentation and nanoassembly by nanorobotic manipulation," *Int. J. Robot. Res.*, vol. 28, no. 4, pp. 537–547, Apr. 2009.

[32] M. J. Gordon, T. Baron, F. Dhalluin, P. Gentile, and P. Ferret, "Size effects in mechanical deformation and fracture of cantilevered silicon nanowires," *Nano Lett.*, vol. 9, no. 2, pp. 525–529, Feb. 2009.

[33] D. Zhang, J.-M. Breguet, R. Clavel, V. Sivakov, S. Christiansen, and J. Michler, "*In situ* electron microscopy mechanical testing of silicon nanowires using electrostatically actuated tensile stages," *J. Microelectromech. Syst.*, vol. 19, no. 3, pp. 663–674, Jun. 2010.

[34] Y.-F. Lin and W.-B. Jian, "The impact of nanocontact on nanowire based nanoelectronics," *Nano Lett.*, vol. 8, no. 10, pp. 3146–3150, Oct. 2008.
[35] A. Asthana, T. Shokuhfar, Q. Gao, P. Heiden, C. Friedrich, and R. S. Yassar, "A study on the modulation of the electrical transport by mechanical straining of individual titanium dioxide nanotube," *Appl. Phys. Lett.*, vol. 97, no. 7, p. 072107, Aug. 2010.
[36] A. Cagliani, R. Wierzbicki, L. Occhipinti, D. H. Petersen, K. N. Dyvelkov, Ö. S. Sukas, B. G. Herstrøm, T. Booth, and P. Bøggild, "Manipulation and *in situ* transmission electron microscope characterization of sub-100 nm nanostructures using a microfabricated nanogripper," *J. Micromech. Microeng.*, vol. 20, no. 3, p. 035009, Mar. 2010.

Xutao Ye received the B.Eng. degree in electrical engineering from the Hong Kong University of Science and Technology, Hong Kong, China, in 2010, and the M.A.Sc. degree in mechanical engineering from the University of Toronto, Toronto, ON, Canada, in 2012.

His research interests include robotics and automation.

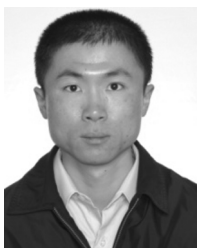

Yong Zhang received the B.S. and M.S. degrees in mechatronics engineering from Harbin Institute of Technology, Harbin, China, in 2005 and 2007, respectively, and the Ph.D. degree in electrical and computer engineering from the University of Toronto, Toronto, ON, Canada, in 2011.

He is currently a Postdoctoral Fellow in the School of Aerospace Engineering, Georgia Institute of Technology, Atlanta, GA, USA. His research interests include the design and fabrication of MEMS devices, micro/nanomanipulation under optical and electron microscopy, and three-dimensional micro/nanomanufacturing.

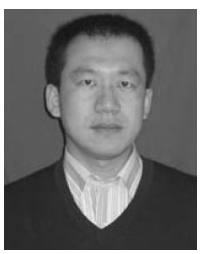

Changhai Ru (M'07) received the Ph.D. degree in mechatronics engineering from Harbin Institute of Technology, Harbin, China, in 2005.

He was a Postdoctoral Fellow in the Department of Mechanical and Industrial Engineering, University of Toronto, Toronto, ON, Canada. He is currently a Professor with the College of Automation, Harbin Engineering University, China. His research interests include micro/nanomanipulation, nanopositioning technologies, and solid-state actuators' driving and control methods.

Jun Luo received the B.S. degree in mechanical engineering from Henan Polytechnic University, Jiaozuo, China, in 1994, the M.S. degree in mechanical engineering from Henan Polytechnic University, Jiaozuo, China, in 1997, and the Ph.D. degree from the Research Institute of Robotics, Shanghai Jiao Tong University, Shanghai, China, in 2000.

He is a Professor with the School of Mechatronic Engineering and Automation, Shanghai University, Shanghai, China. He is the Head of Precision Mechanical Engineering Department, Shanghai University, and the Vice Director of Shanghai Municipal Key Laboratory of Robotics. His research areas include robot sensing, sensory feedback, mechatronics, man-machine interfaces, and special robotics.

Shaorong Xie received the B.S. and M.S. degrees in mechanical engineering from Tianjin Polytechnic University, Tianjin, China, in 1995 and 1998, respectively, and the Ph.D. degree in mechanical engineering from the Institute of Intelligent Machines at Tianjin University and the Institute of Robotics and Automatic Information System, Nankai University, Nankai, China, in 2001.

She is a Professor with the School of Mechatronic Engineering and Automation, Shanghai University, Shanghai, China. Her research areas include advanced robotics technologies, bionic control mechanisms of eye movements, and image monitoring systems.

Yu Sun (S'01–M'03–SM'07) received the B.S. degree in electrical engineering from Dalian University of Technology, Dalian, China, in 1996, the M.S. degree from the Institute of Automation, Chinese Academy of Sciences, Beijing, China, in 1999, and the M.S. degree in electrical engineering and the Ph.D. degree in mechanical engineering from the University of Minnesota, Minneapolis, MN, USA, in 2001 and 2003, respectively.

He is a Professor with the Department of Mechanical and Industrial Engineering and is jointly appointed with the Institute of Biomaterials and Biomedical Engineering and the Department of Electrical and Computer Engineering, University of Toronto, Toronto, ON, Canada. He is the Canada Research Chair in Micro and Nano Engineering Systems. His research areas include the design and fabrication of M/NEMS devices, micronanorobotic manipulation, and the manipulation and characterization of cells, biomolecules, and nanomaterials.